THE JOURNAL OF PHYSICAL CHEMISTRY A

Article

pubs.acs.org/JPCA

Photofragmentation Mechanisms of Chlorosulfonyl Isocyanate, $ClSO_2NCO$, Excited with Synchrotron Radiation between 12 and 550 eV

Angélica Moreno Betancourt,[†] Yanina B. Bava,[†] Yanina Berrueta Martínez,[†] Mauricio F. Erben,[†] Reinaldo L. Cavasso Filho,[‡] Carlos O. Della Védova,[†] and Rosana M. Romano*[,†]

[†]CEQUINOR (UNLP−CONICET, CCT La Plata), Departamento de Química, Facultad de Ciencias Exactas, Universidad Nacional de La Plata, CC 962, La Plata CP 1900, Argentina

[‡]Universidade Federal do ABC, Rua Catequese, 242, CEP 09090-400, Santo André, São Paulo, Brazil

ABSTRACT: The unimolecular photofragmentation mechanisms of chlorosulfonyl isocyanate, $ClSO_2NCO$, excited with tunable synchrotron radiation between 12 and 550 eV, were investigated by means of time-of-flight (TOF) coincidence techniques. The main fragmentation mechanism after single ionization, produced by irradiation of an effusive beam of the sample with synchrotron light in the valence electron region, occurs through the breaking of the Cl−S single bond, giving a chloride radical and a SO_2NCO^+ fragment. This mechanism contrasts with the one observed for the related FSO_2NCO, in which the rupture of the S−N bond originates the FSO_2^+ fragment. The energies of the shallow- (S 2p, Cl 2p, and S 2s) and core-shell (C 1s, N 1s, and O 1s) electrons were determined by X-ray absorption. Transitions between these shallow and core electrons to unoccupied molecular orbitals were also observed in the total ion yield (TIY) spectra. Fourteen different fragmentation mechanisms of the doubly charged parent ion, $ClSO_2NCO^{2+}$, were inferred from the bidimensional photoelectron-photoion-photoion-coincidence (PEPIPICO) spectra. The rupture of the S−N bond can evolve to form $NCO^+/SO_2^{\bullet+}$, $NCO^+/SO^{\bullet+}$, or $S^{\bullet+}/NCO^+$ pairs of ions. The Cl−S bond breaking originates different mechanisms, $Cl^+/SO^{\bullet+}$, $Cl^+/S^{\bullet+}$, $CO^{\bullet+}/S^{\bullet+}$, $O^{\bullet+}/SO^{\bullet+}$, $O^{\bullet+}/Cl^+$, $O^{\bullet+}/S^{\bullet+}$, $C^{\bullet+}/S^{\bullet+}$, and $C^{\bullet+}/O^{\bullet+}$ pairs being detected in coincidence as the final species. Another three coincidence islands can only be explained with an initial atomic rearrangement forming $ClNCO^{2+}$, $ONCO^{2+}$, and $ClCO^{2+}$, as precursors of $CO^{\bullet+}/Cl^+$, $O^{\bullet+}/CO^{\bullet+}$, and $C^{\bullet+}/Cl^+$ pairs, respectively. The formation of $Cl^\bullet$ radical is deduced from several mechanisms.

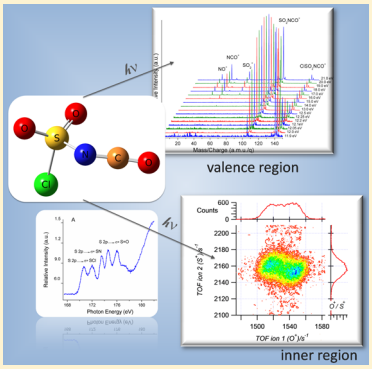

INTRODUCTION

During the past years our research group has been interested in photochemical studies of small molecular compounds, using either nonionizing light or ionizing radiation (see for example refs 1−4 and references cited therein). The aim of these investigations is the elucidation of the photochemical mechanisms in a wide spectral energy range, and the detection of reactive intermediates. Photolysis with nonionizing light leads to free radical and neutral molecules, for identification of which matrix-isolation IR spectroscopy is a very well suited technique. On the other hand, the charged species produced by ionizing radiation can be detected with time-of-flight (TOF) spectrometry. Particularly, coincidence techniques are very useful for the study of fragmentation mechanisms of molecules after multiple ionization processes (see for example refs 1, 20, and 25 and references cited therein). By detecting the fragment ions it is possible not only to determine the dynamic of the fragmentation process but also to infer the nature of the final cationic species produced after the Auger decay. A synchrotron source is ideal for these investigations, as it provides high-intensity tunable radiation in a wide energy range.

In a previous paper our research group has reported the photolysis of chloro- and fluorosulfonyl isocyanate, $ClSO_2NCO$ and FSO_2NCO, with nonionizing radiation in the energy range between 800 and 200 nm (1.5 to 6.2 eV).[5] The photolysis of $ClSO_2NCO$ isolated in Ar and N_2 solid matrixes leads to the quantitative formation of a 1:1 molecular complex between SO_2 and ClNCO. On the other hand, the related FSO_2NCO species is almost photostable in the same conditions. The ionic fragmentation mechanisms of FSO_2NCO using synchrotron radiation between 10 and 1000 eV was recently studied.[6] The FSO_2^+ ion, formed from the breaking of the S−N single bond, was the most intense fragment when the sample was irradiated with energy in the electronic valence region. At the shallow- and core-level energy regions, different fragmentation pathways were opened, the most important ones being secondary decay after deferred charge separation (SD-DCS) mechanisms leading to the formation of the $O^{\bullet+}/S^{\bullet+}$ and $C^{\bullet+}/O^{\bullet+}$ pairs. However, as far as we know, no photochemical studies in the valence and

Received: March 11, 2015
Revised: June 26, 2015
Published: June 29, 2015

DOI: 10.1021/acs.jpca.5b02396
J. Phys. Chem. A 2015, 119, 8021−8030

shallow- and core-level electronic energy regions were reported for the congener $ClSO_2NCO$.

Chlorosulfonyl isocyanate is a reactant extensively used in pharmaceutical synthesis and also as a precursor of herbicide and pesticide products.[7] The conformational and bond properties of $ClSO_2NCO$ were determined by vibrational spectroscopy, including Raman depolarization measurements.[8,9] Only one structure with *gauche* conformation was detected for the gas phase, in agreement with gas electron diffraction measurements.[10] The outermost electronic structure of chlorosulfonyl isocyanate was studied by He(I) photoelectron spectroscopy (PES).[11] The first ionization potential was determined to be at 12.02 eV. The authors concluded that the photoelectron spectrum of $ClSO_2NCO$ suggests a significant effect of the interactions between chlorine "lone-pair" electrons and the NCO group on the energy and character of the HOMO.

In this paper we present the study of the unimolecular photofragmentation mechanisms of $ClSO_2NCO$ after single and double ionization using coincidence techniques and synchrotron tunable radiation between 10 and 550 eV. Ionization energies of shallow and core electrons of the molecule, and also electronic transitions from these electronic levels to unoccupied molecular orbitals (LUMOs), were determined by recording total ion yield (TIY) spectra as a function of the energy of the incident synchrotron light. Fragmentation mechanisms in the valence energy region, after single ionization, were studied by means of the photoelectron-photoion-coincidence (PEPICO) technique. The dynamic of the fragmentations that follows a doubly ionization process was inferred from the bidimensional photoelectron-photoion-photoion-coincidence (PEPIPICO) spectra.

EXPERIMENTAL SECTION

Sample. $ClSO_2NCO$ was obtained from a commercial source (Aldrich) and purified by several trap-to-trap distillations under vacuum conditions. The purity of the vapor phase of the sample was corroborated by comparison of the FTIR spectrum with the reported one.[8]

Synchrotron Measurements. Synchrotron radiation was used at the Laboratório Nacional de Luz Síncrotron (LNLS), Campinas, Sao Paulo, Brazil.[12] Linearly polarized light monochromatized by a toroidal grating monochromator (available at the TGM bending magnet beamline in the range 10−310 eV) or a spherical grating monochromator (available at the SGM bending magnet beamline in the range 200−1000 eV)[13] intersects the effusive gaseous sample inside a high-vacuum experimental station[14] at a base pressure in the range of 10^{-8} mbar. During the experiments, the pressure was maintained below 2×10^{-6} mbar. The resolution power is better than 400 in the TGM beamline, reaching an $E/\Delta E = 550$ in the range from 10 to 21.5 eV. High-purity vacuum-ultraviolet photons are used. The problem of contamination by high-order harmonics in the low-energy region, between 10 and 21.5 eV, was suppressed by the gas-phase harmonic filter installed in the TGM beamline at the LNLS.[15−17] The first ionization threshold of neon at 21.56 eV, used as filtering gas, was employed to calibrate the photon energy and bandwidth of the beamline. The resolution of the photon energy calibration is better than the line width, ΔE. The energy calibration for the 100−310 eV energy region was established by means of the S 2p → $6a_{1g}$ and S 2p → $2t_{2g}$ absorption resonances in SF_6.[18] In the SGM beamline the resolution is $\Delta E/E < 200$. The intensity of the emergent beam was recorded by a light-sensitive diode. The ions produced by the interaction of the gaseous sample with the light beam were detected by means of a TOF mass spectrometer of the Wiley−McLaren type for both PEPICO and PEPIPICO measurements.[19,20] This instrument was constructed at the Institute of Physics, Brasilia University, Brasilia, Brazil.[21] The axis of the TOF spectrometer is perpendicular to the photon beam and parallel to the plane of the storage ring. Electrons are accelerated to a multichannel plate (MCP) and recorded without energy analysis. This event starts the flight time determination process for the corresponding ion, which was consequently accelerated to another MCP. Total ion yield (TIY) measurements were performed with an energy pass of 0.1 eV and acquisition time of 5 s, and 3 spectra were averaged to improve the signal/noise ratio.

Theoretical Calculations. NBO calculations using the B3LYP/6-311+G(d) level of approximation at the optimized geometry of the most stable *gauche* conformer of $ClSO_2NCO$ in its ground electronic state have been performed using the Gaussian03 program package.[22] The energies of the possible fragments arising from the dissociation of the $ClSO_2NCO^{\bullet+}$ parent radical ion were calculated, using the UB3LYP/6-311+G(d) level of approximation.

RESULTS AND DISCUSSION

Photoexcitation, Photoionization, and Photofragmentation Mechanisms with Synchrotron Radiation in the Valence Energy Region. An effusive beam of $ClSO_2NCO$, maintained below 2×10^{-6} mbar, was excited with monochromatic synchrotron radiation, with energies between 10 and 21 eV. The positive ion formed after photoionization and/or photofragmentation of the molecule was detected in coincidence with the ejected electron, using the PEPICO technique. Each unimolecular mechanism, guaranteed by the low pressure of the sample inside the chamber, originates a signal in the spectrum, corresponding to the time of flight of the positive ion, proportional to its m/z ratio.

Figure 1 shows the PEPICO spectra, normalized with respect to the sum of the areas of all peaks, measured at selected photon energies corresponding to the ionization of valence electrons. A list of the positive ions, their assignment, and their relative abundances (%) as a function of the energy of the incident

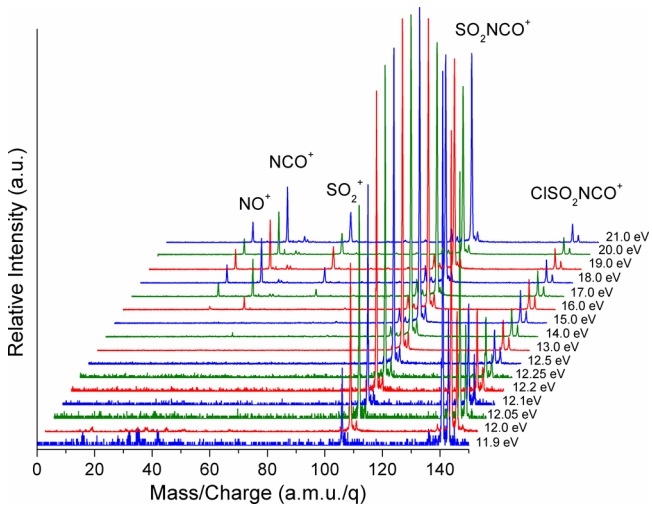

Figure 1. PEPICO spectra of $ClSO_2NCO$ taken at different irradiation synchrotron light in the valence energy region, between 11.9 and 21.0 eV.

DOI: 10.1021/acs.jpca.5b02396
J. Phys. Chem. A 2015, 119, 8021−8030

Table 1. Integrated Areas (%) of Positive Ions Extracted from PEPICO Spectra as a Function of the Photon Energies between 11.9 and 21.0 eV for $ClSO_2NCO$

		photon energy (eV)															
m/z	ion	11.9	12.0	12.05	12.1	12.2	12.25	12.5	13.0	14.0	15.0	16.0	17.0	18.0	19.0	20.0	21.0
30	NO^+											1.8	4.8	6.0	6.6	7.0	6.9
42	NCO^+											3.6	9.5	12.8	14.3	13.7	15.7
48	$SO^{\bullet+}$												0.9	1.3	1.6	2.5	2.2
49	$ClN^{\bullet+}$												0.8	1.0	1.2	1.8	1.1
64	$SO_2^{\bullet+}$												2.1	5.0	8.1	9.4	10.7
83	$ClSO^+$															2.5	1.2
90	SO_2NC^+															2.5	1.3
99	$ClSO_2^+$									4.2	7.0	6.5	6.4	6.2	5.9	6.5	5.5
106	SO_2NCO^+	10.1	27.6	40.7	52.9	72.2	75.1	86.2	89.5	86.9	84.7	79.3	68.4	61.3	56.6	47.5	50.4
141	$ClSO_2NCO^{\bullet+}$	89.9	72.4	59.3	47.1	27.8	24.9	13.8	10.5	8.9	8.3	8.6	6.9	6.3	5.8	6.6	5.0

radiation is presented in Table 1 (only fragments that contribute with more than 0.1% were included in the table). The fragments containing a chlorine atom are clearly identified by their characteristic signals originated in the isotopologues of ^{35}Cl and ^{37}Cl, as can be appreciated in Figure 1. The signals of fragments containing a sulfur atom, particularly the ones with appreciable intensities, present a satellite corresponding to ^{34}S. The relative intensities listed in Table 1 correspond to the sum of the abundances of the naturally occurring isotopologues for each fragment.

When the sample was irradiated with photons of energy below 11.9 eV, neither ions nor electrons were detected. This result is consistent with the value of the first ionization potential of $ClSO_2NCO$, determined at 12.02 eV by photoelectron spectroscopy.[10] At 11.9 eV, the lowest energy that produces ionization, the PEPICO spectrum is dominated by the parent ion ($M^{\bullet+}$), denoting events of ionization without subsequent fragmentation. Only approximately 10% of the ionized molecules suffer a fragmentation through the rupture of the Cl−S single bond after ionization, giving SO_2NCO^+ and $Cl^\bullet$ eq 1.

$$ClSO_2NCO^{\bullet+} \rightarrow Cl^\bullet + SO_2NCO^+ \quad (1)$$

The unimolecular mechanism described by eq 1 is the most important fragmentation channel at all the studied energies in the valence region, as can be observed in Figure 1, and also in Figure 2, that depicts the branching ratios of the most abundant ions in the PEPICO spectra of $ClSO_2NCO$ as a function of the irradiation energy. On the other hand, the main photofragmentation mechanism of the related FSO_2NCO molecule excited in the valence electron energy region is the rupture of the S−N bond, which originates the FSO_2^+ fragment.[6] This difference may be related to the character of the HOMOs of both molecules, determined by photoelectron spectroscopy and theoretical calculations.[6,11] While the HOMO and HOMO − 1 of $ClSO_2NCO$ were assigned to electron lone pairs formally located on the chlorine atom,[10] justifying the tendency to the rupture of the Cl−S bond after ionization with low-energy light, the HOMO and HOMO − 1 of FSO_2NCO can be considered mainly as π_{NCO} nonbonding orbitals.[6] In addition, a topological electron density analysis of $ClSO_2NCO$ was previously reported, assigning a weak ionic character to the Cl−S bond.[10]

The signal assigned to $ClSO_2^+$ is observed in the spectra of $ClSO_2NCO$ taken with $E \geq 14$ eV with very low abundances, between 4 and 7% depending on the excitation energy (see Table 1). As mentioned in the previous paragraph, the fragmentation through the S−N bond is the main mechanism for the analogous FSO_2NCO.[6] From 16 eV, the NCO^+ ion is detected in the

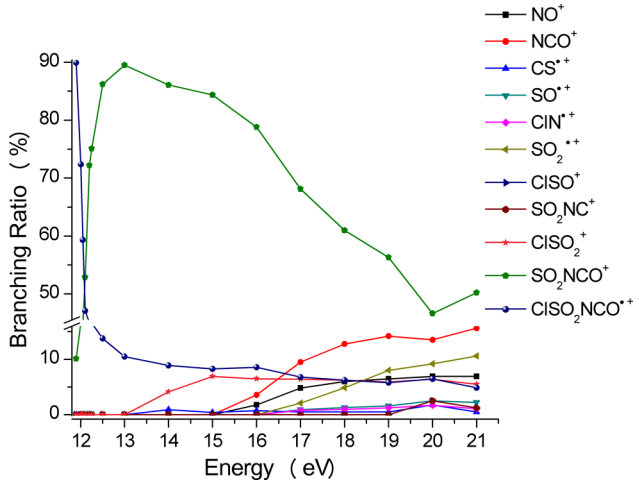

Figure 2. Branching ratios (%) for fragment ions extracted from PEPICO spectra as a function of the photon energies between 11.9 and 21.0 eV for $ClSO_2NCO$.

spectra and its abundance grows with the excitation energy, until it converts to the second most abundant fragment at 21 eV (see Figure 2). The $SO_2^{\bullet+}$ species is visible from 17 eV, and it turns out also to be one of the most abundant fragments at higher energies. The formation of this ion can be explained only by the rupture of, at least, two bonds. As the excitation energy increases, $ClN^{\bullet+}$ and NO^+ fragments, arising from intramolecular rearrangement processes, are detected in the spectra.

The experimental fragmentation mechanisms were contrasted with the theoretical energy differences between possible fragments and the parent ion, calculated with the UB3LYP/6-311+G(d) approximation. In these calculations only fragmentations involving the rupture of one molecular bond and originating only one neutral fragment were modeled. The energetics of two of the most relevant mechanisms, the rupture of the Cl−S and S−N bonds, are represented in Scheme 1. For each mechanism the energies of the two possible situations after the fragmentation, depending on which of the fragments retains the positive charge, are depicted in the scheme. According to the calculations, the rupture of the Cl−S bond energetically favors the formation of SO_2NCO^+ instead of Cl^+, by more than 5 eV. Even more, the energy of the fragmentation channel leading to the formation of $Cl^\bullet$ + SO_2NCO^+ is predicted only 0.21 eV higher than $M^{\bullet+}$. This result is in complete agreement with the experimental findings, since the SO_2NCO^+ ion is the most

DOI: 10.1021/acs.jpca.5b02396
J. Phys. Chem. A 2015, 119, 8021−8030

Scheme 1. Relative Energies for Different Possible Fragmentation Mechanisms of $ClSO_2NCO^{\bullet+}$ Calculated with the UB3LYP/6-311+G(d) Approximation

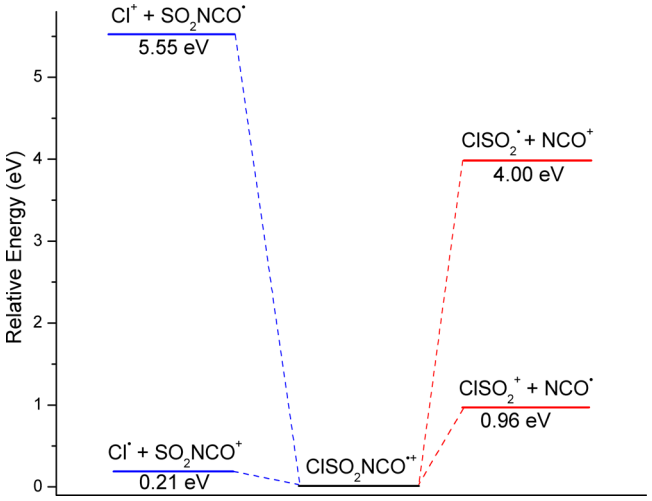

abundant one, even at energies just above the first ionization potential.

For the second mechanisms, corresponding to the fragmentation through the S−N bond, the calculations also qualitatively reproduce the experiments, predicting the $ClSO_2^+$ fragment, which appears at lower energy in the PEPICO spectra, more favorable than the NCO^+ ion. However, and considering the relatively high proportion of the NCO^+ fragment at higher energies (ca. 15% at 21 eV), their formation from secondary mechanisms, as for example the fragmentation of SO_2NCO^+, cannot be discarded. As can be observed in Table 1, the increase of the intensity of NCO^+ is accompanied by the decrease of the SO_2NCO^+ fragment, and also of the appearance of $SO_2^{\bullet+}$, reinforcing the idea that these species can arise from the rupture of the SO_2−NCO^+ ion through the S−N bond.

Photoionization and Photofragmentation with Synchrotron Radiation in the Shallow- and Core-Level Energy Regions. The use of tunable synchrotron radiation in a wide energy range allows the study of the fragmentation mechanisms as specific electrons are excited and/or ionized. The first step of this study is then the localization of these energies, by recording the total ion yield (TIY) spectra as a function of the incident synchrotron energy. Figure 3 shows TIY spectra in selected regions, corresponding to the excitation of electrons located at the S 2p, Cl 2p, S 2s, C 1s, N 1s, and O 1s levels.

Five well-defined peaks are observed before the ionization of S 2p electrons, at 170.3, 171.6, 173.2, 174.2, and 175.6 eV (Figure 3A). These bands can be assigned to resonant electronic excitations from $2p_{1/2}$ and $2p_{3/2}$ levels to unoccupied molecular orbitals. To help in the interpretation and tentative assignment of these transitions, the energetic order and main character of LUMOs of the fundamental electronic state of the main conformer of $ClSO_2NCO$ were predicted with the NBO-B3LYP/6-311+G(d) approximation. The first eight LUMOs are depicted in Figure 4. The 170.5 eV band was then tentatively assigned to the S $2p_{3/2}$ → σ^*S−Cl transition. The other four peaks may be explained as transitions from S $2p_{3/2}$ to σ^* S−N (LUMO + 3) and σ^* S═O (LUMO + 4 and LUMO + 5) overlapped with the excitation of electrons from the S $2p_{1/2}$ level to the same LUMOs. An energy difference between the S $2p_{1/2}$ and $2p_{3/2}$ of around 1.3 eV, together with a 1:2 intensity ratio, is expected for SO_2 containing compounds (see for example refs 23 and 24 for sulfur dioxide and dimethyl sulfoxide, respectively).

In the Cl 2p energy region, only one resonance was observed as a low-intensity and broad band at approximately 208 eV (Figure 3B). This signal was assigned with confidence to the Cl 2p → σ^*S−Cl transition. The ionization the Cl 2p threshold occurs at ca. 214.7 eV. A unique and unstructured band at 238.7 eV (Figure 3C) corresponds to the ionization of S 2s electrons.

The TIY spectrum in the C 1s region depicted in Figure 3D is almost identical with the one obtained for the related FSO_2NCO,[6] indicating that the molecular orbitals involved in the resonance are almost independent of the terminal halogen, Cl or F. Below the C 1s threshold, near 292 eV, the spectrum is dominated by two strong signals at 287.9 and 289.1 eV attributed to the C 1s → π^* C═O (LUMO+1) and C 1s → π^* C═O (LUMO + 2).

Figure 3E shows the TIY spectrum of $ClSO_2NCO$ in the energy region of the excitation and ionization of N 1s electrons. The ionization threshold is close to 408 eV, preceded by a complex structure with bands at 398.9, 400.2, 400.9, 403.3, and 404.3 eV. These signals can be assigned mainly to N 1s → σ^* S−N (LUMO + 3) and N 1s → σ^* N═C (LUMO + 7) transitions. It is also probable that some of them can be attributed to excitations to π^* C═O molecular orbitals, due to a delocalization of these orbitals over the nitrogen atom.

The TIY spectrum in the O 1s region, shown in Figure 3F, presents at least two resonances located at 535.4 and 536.9 eV, although the shape of the second band would indicate the overlap with at least a third band. Due to the presence of nonequivalent oxygen atoms in the molecule, the assignment is not trivial, but a plausible explanation for these resonances could be O 1s → π^* C═O (LUMO + 1), O 1s → π^* C═O (LUMO + 2) and O 1s → σ^* S═O (LUMO + 4 and LUMO + 5) transitions.

Once the resonant excitation and ionization energies were detected, the study of fragmentation mechanisms, and their dependence with the incident light energy, was performed by recording the positive ions originated in each fragmentation event. At these shallow- and core-level energies, both single and also double ionization processes are feasible. The single-charged positive fragments detected in the PEPICO mode may proceed for the fragmentation of either M^+ or M^{+2} (but fragments with $m/z > M/2$ can arise only from M^+ because in PEPICO spectra only the lighter ion is detected). On the other hand, in the PEPIPICO mode two positive ions originated in the same fragmentation event are detected in coincidence, constituting a very important tool for the study of fragmentation mechanisms.

Table 2 lists the relative intensities of the positive fragments observed in the PEPICO spectra taken at selected energies in the whole range investigated, that correspond to some of the resonances and ionization thresholds previously described, and also off-resonance energies, presented in increasing energy order. Figures 5 and 6 show some of the PEPICO spectra taken at different photon energies. As explained in the previous paragraph, the fragments SO_2NCO^+, $ClSO_2^+$, SO_2NC^+, and $ClSO_2^+$ can arise only from fragmentation of a single-charged parent ion. According to the relative intensities of these ions, the rupture of the Cl−S bond remains as the most favored fragmentation mechanism for the single-charged parent ion, as concluded for the excitation of the molecule in the valence energy region.

The ions with $m/z \leq 64$ may correspond to fragments derived from $M^{\bullet+}$, M^{2+}, or both. As we will discuss later in this paper, a complete analysis of these contributions can be realized through

DOI: 10.1021/acs.jpca.5b02396
J. Phys. Chem. A 2015, 119, 8021−8030

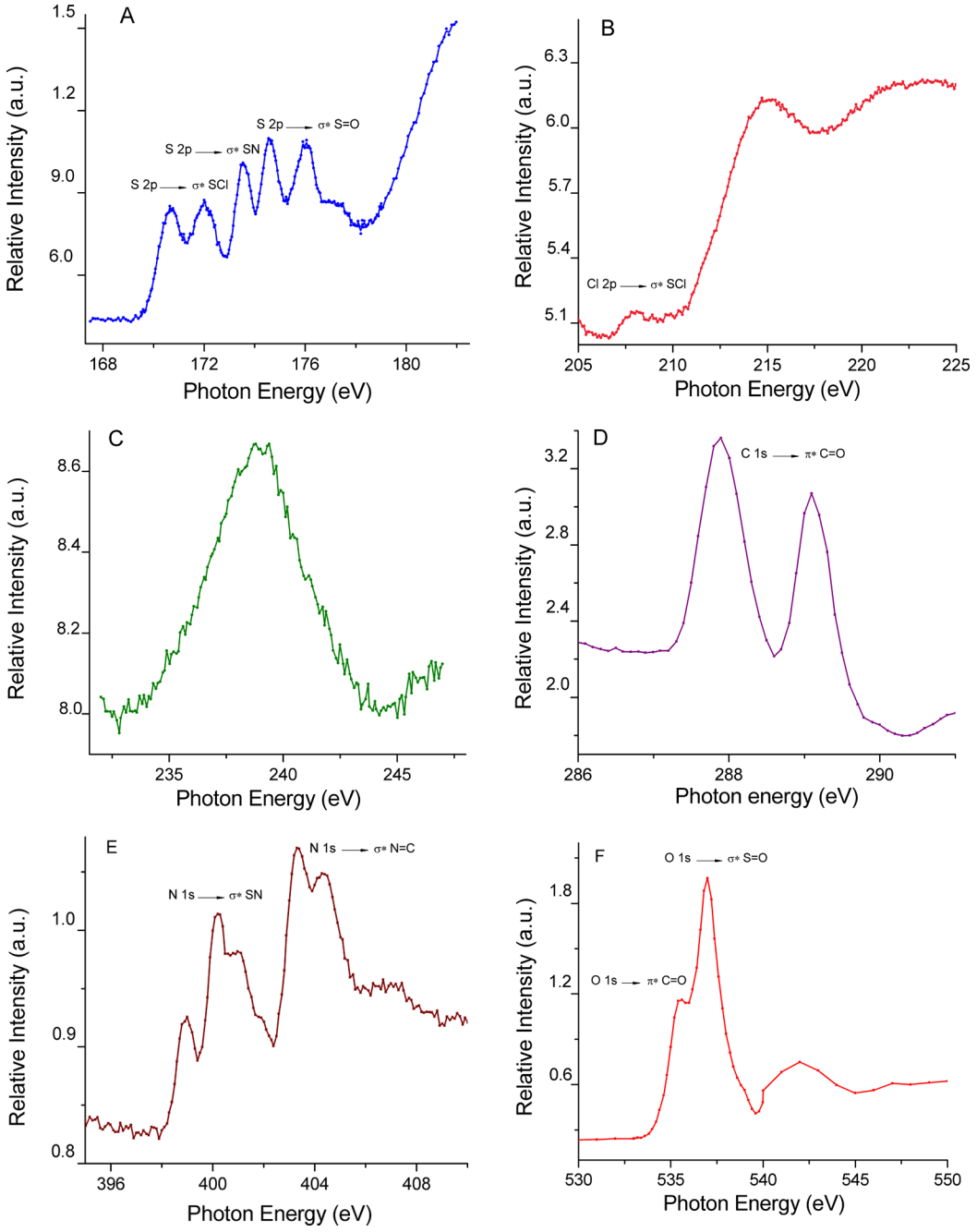

Figure 3. Total ion yield (TIY) spectra of $ClSO_2NCO$ in the S 2p (A), Cl 2p (B), S 2s (C), C 1s (D), N 1s (E), and O 1s (F) energy regions.

the PEPIPICO spectra and their T_1 (time of flight of the lighter ion) and T_2 (time of flight of the second lighter ion) projections. A clear difference of the spectra taken with excitation in the shallow- and core-shell electron energy regions with respect to the ones taken in the valence energy region is the presence of atomic fragments (all the atoms of the molecule appears as cations: $C^{\bullet+}$, N^+, $O^{\bullet+}$, $S^{\bullet+}$, and Cl^+). On the other hand, the doubly charged fragments, C^{2+}, O^{2+}, $Cl^{\bullet 2+}$, and CS^{2+}, are observed only in the spectra taken with light in the core-level regions. The formation of the last of these species, CS^{2+}, and also NO^+ and $CS^{\bullet+}$ fragments, necessarily requires a rearrangement process. However, $ClN^{\bullet+}$, a species formed through an atomic rearrangement when the sample was irradiated with light in the valence energy region from energies of 17 eV, was absent in the shallow and core regions.

As shown in Table 2 and qualitatively observed in Figures 5 and 6, a gradual increase of the atomic fragments is evident as the incident energy increases. Besides this gradual change, a clear difference in the ion branching ratios is observed in the spectrum taken when the incident photon energy is tuned on the O(1S) resonance. While $C^{\bullet+}$, $O^{\bullet+}$, and $CO^{\bullet+}$ fragments increase their intensities with respect to the average values at the other energies (see Table 2), $Cl^{\bullet+}$, NCO^+, and to less extent $S^{\bullet+}$ decrease with respect to the main values, denoting a moderated site-specific effect for the PEPICO spectrum taken in the O(1s) region.

The relative intensities of the coincidences between two positive ions originated in the fragmentation of the M^{2+} parent ion, extracted from the bidimensional PEPIPICO spectra taken at selected energies, are presented in Table 3. Although it is not possible to find a clear behavior of the relative intensities of the

DOI: 10.1021/acs.jpca.5b02396
J. Phys. Chem. A 2015, 119, 8021−8030

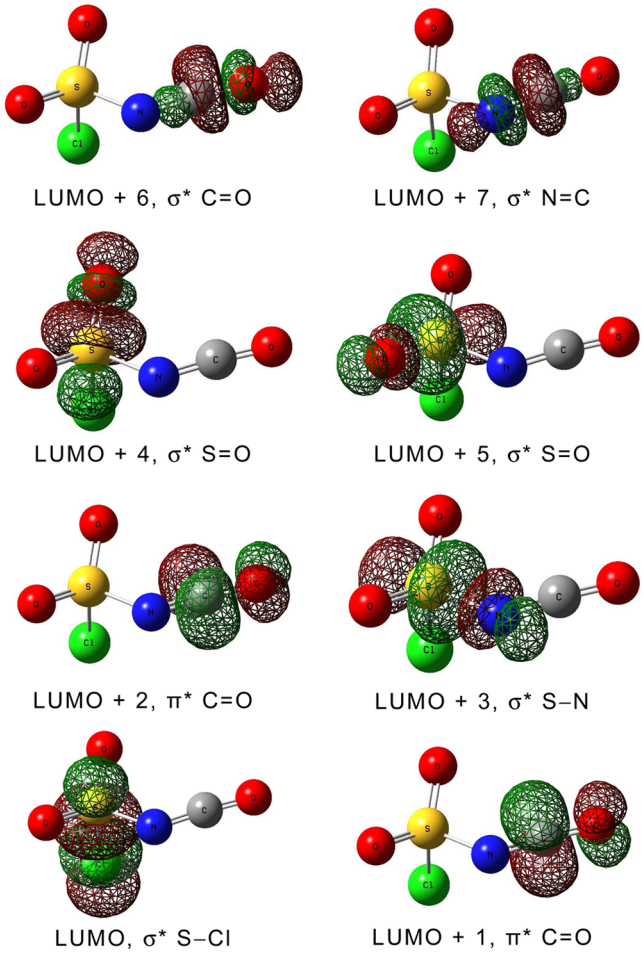

Figure 4. Schematic representation and approximate assignment of the eight lowest unoccupied molecular orbitals of $ClSO_2NCO$ calculated with the B3LYP/6-311+G(d) approximation.

coincidence islands with the ionization energy, some peculiarities are worth being mentioned. For example, the two coincidences in which one fragment contains a sulfur atom and the other a chlorine atom, $Cl^+/SO^{\bullet+}$ and $S^{\bullet+}/Cl^+$, were relatively enhanced when S or Cl shallow-shell electrons were excited (see Table 3). On the other hand, more than 85% of the coincidences observed in the PEPIPICO spectrum excited with 535.4 eV, in resonance with the O 1s → π^* C═O electronic transition, contain $O^{\bullet+}$ as one of the fragments, the coincidence $C^{\bullet+}/O^{\bullet+}$ being 45.5% abundant. Another interesting feature of the spectra is the coincidences between all possible atomic fragments ($C^{\bullet+}/O^{\bullet+}$, $C^{\bullet+}/S^{\bullet+}$, $C^{\bullet+}/Cl^+$, $O^{\bullet+}/S^{\bullet+}$, $O^{\bullet+}/Cl^+$, and $S^{\bullet+}/Cl^+$), with the only exception of the N^+, that is not observed to arrive in coincidence with any other species, at least with appreciable intensity.

Although the relative intensities of the coincidences depend on the excitation energy, as can be observed in Table 3, the shape and slope of the islands, that contain valuable information about the dynamic of the fragmentation processes, are independent of the energy, indicating that the mechanisms are the same in all the energy range investigated. Following the formalisms proposed by Eland,[25] based on the requirement of the linear momentum conservation of the fragments, the experimental shape and slope of the coincidence islands in the PEPIPICO spectra were compared with the theoretical slopes of the different possible mechanisms for each coincidence. The results are presented below. In all the cases the islands observed in the PEPICO spectra present a parallelogram shape.

$NCO^+/SO_2^{\bullet+}$ Coincidence. Although this coincidence is not one of the most abundant, it involves the heaviest fragments and then allows the unambiguous elucidation of the fragmentation mechanism. Starting from M^{2+}, three different fragmentation mechanisms are feasible. The first possibility is a concerted mechanism, as described in eq 2.

$$ClSO_2NCO^{2+} \rightarrow Cl^{\bullet} + \mathbf{SO_2}^{\bullet+} + \mathbf{NCO}^{+} \quad (2)$$

Following the formalisms proposed by Eland, an ovoid-shape is expected for this coincidence. The second possible mechanism, represented by eq 3, corresponds to a deferred charge separation (DCS) mechanism, starting with the loss of a chlorine atom.

$$ClSO_2NCO^{2+} \rightarrow Cl^{\bullet} + SO_2NCO^{\bullet 2+}$$
$$SO_2NCO^{\bullet 2+} \rightarrow \mathbf{SO_2}^{\bullet+} + \mathbf{NCO}^{+} \quad (3)$$

The expected shape of the island originated by the mechanisms described by eq 3 is a parallelogram with a −1 slope. The last possible mechanism corresponds to a secondary decay (SD) as presented in eq 4.

$$ClSO_2NCO^{2+} \rightarrow ClSO_2^{+} + \mathbf{NCO}^{+}$$
$$ClSO_2^{+} \rightarrow Cl^{\bullet} + \mathbf{SO_2}^{\bullet+} \quad (4)$$

The theoretical slope for this mechanism is −1.5. The comparison with the experimental island of the $NCO^+/SO_2^{\bullet+}$ coincidence, with a parallelogram shape and an approximate slope of −1, allows us to conclude that the DCS mechanism described by eq 3 is responsible for this coincidence. It is interesting to note that the formation of the NCO^+ and $SO_2^{\bullet+}$ fragments in coincidence was not observed for the analogous molecules FSO_2NCO. As mentioned earlier, the rupture of the Cl−S bond as initiator of the mechanism may be the difference with the fluorinated compound.

$NCO^+/SO^{\bullet+}$ Coincidence. The −1 experimental slope of this coincidence island cannot be undoubtedly determined, since at least two different mechanisms can account for this slope. However, considering the tendency to the rupture of the Cl−S bond, the following four-body DCS mechanism can be proposed:

$$ClSO_2NCO^{2+} \rightarrow Cl^{\bullet} + SO_2NCO^{\bullet 2+}$$
$$SO_2NCO^{\bullet 2+} \rightarrow O + OSNCO^{\bullet 2+}$$
$$OSNCO^{\bullet 2+} \rightarrow \mathbf{SO}^{\bullet+} + \mathbf{NCO}^{+} \quad (5)$$

$Cl^+/SO^{\bullet+}$ Coincidence. The relative intensity of this coincidence decreases as the energy of the incident radiation increases, from ∼9% at 182.8 eV to 2% at 535.4 eV. The contour map of the $Cl^+/SO^{\bullet+}$ island recorded at 403.4 eV is shown in Figure 7, in which a satellite corresponding to the $^{37}Cl^+/SO^{\bullet+}$ coincidence can be observed. The experimental slope of approximately −0.75 can be explained by a secondary decay after a deferred charge separation (SD-DCS) mechanism described by eq 6, with a −0.75 theoretical slope.

$$ClSO_2NCO^{2+} \rightarrow ClSO_2^{\bullet 2+} + NCO^{\bullet}$$
$$ClSO_2^{\bullet 2+} \rightarrow \mathbf{Cl}^{+} + SO_2^{\bullet+}$$
$$SO_2^{\bullet+} \rightarrow O + \mathbf{SO}^{\bullet+} \quad (6)$$

DOI: 10.1021/acs.jpca.5b02396
J. Phys. Chem. A 2015, 119, 8021−8030

Table 2. Integrated Areas (%) of Positive Ions Extracted from PEPICO Spectra of $ClSO_2NCO$ as a Function of Selected Photon Energies in the S 2p, Cl 2p, S 2s, C 1s, N 1s, and O 1s Energy Regions[a]

		photon energy (eV)												
m/z[b]	ion	170.5	171.6	174.2	175.6	202.0	207.8	214.7	238.7	270.0	280.0	287.9	403.4	535.4
6	C^{2+}									0.5		0.3	0.5	0.7
8	O^{2+}									1.9		1.5	2.0	2.8
12	$C^{\bullet+}$	2.8	2.9	3.2	3.3	3.9	3.7	3.1	3.6	4.3	3.7	4.4	4.9	14.6
14	N^+	3.5	3.5	3.9	4.0	4.5	4.4	3.7	4.1	4.7	4.1	5.1	5.3	3.1
16	$O^{\bullet+}$	7.6	7.6	8.4	8.7	12.9	12.1	10.2	12.2	17.1	14.0	17.7	18.7	28.3
17.5	$Cl^{\bullet2+}$									0.9		0.7	0.9	0.8
22	CS^{2+}									0.4		0.3	0.4	0.4
26	CN^+	3.1	3.3	3.5	3.5	3.9	3.7	3.3	3.4	3.4	3.3	3.3	3.5	2.0
28	$CO^{\bullet+}$	5.7	5.9	6.4	6.4	7.4	7.2	6.3	6.7	5.9	6.9	6.3	5.9	13.3
30	NO^+	3.4	3.4	3.3	3.2	2.7	2.7	2.9	2.6	1.6	2.5	1.7	1.5	1.1
32	$S^{\bullet+}$	8.7	8.7	9.6	9.6	10.9	10.8	9.3	10.4	10.0	10.7	10.6	10.5	6.2
35	Cl^+	16.3	16.5	16.9	17.0	18.9	19.3	22.0	21.5	22.1	22.1	21.7	20.9	11.2
42	NCO^+	9.8	9.6	8.7	8.7	7.9	7.9	10.7	9.7	8.9	10.0	8.7	7.8	4.0
44	$CS^{\bullet+}$	0.8	0.8	0.9	0.9	0.8	0.8	0.7	0.7	0.7	0.5	0.6	0.7	1.1
46	SN^+	4.3	4.2	4.1	3.9	3.6	3.7	3.5	3.3	2.7	3.0	2.7	2.5	1.8
48	$SO^{\bullet+}$	10.9	10.7	10.6	10.3	8.6	9.8	9.0	8.4	7.5	8.5	8.6	7.8	5.4
64	$SO_2^{\bullet+}$	6.4	6.3	5.6	5.7	4.0	4.2	5.4	4.6	3.2	4.2	3.4	2.9	1.8
83	$ClSO^+$	1.5	1.5	1.6	1.5	1.2	1.1	1.1	1.0	0.6	0.6	0.4	0.6	0.3
90	SO_2NC^+	1.6	1.6	1.6	1.5	1.3	1.2	1.3	1.2	0.6	0.8	0.3	0.6	0.2
99	$ClSO_2^+$	2.7	2.8	2.7	2.7	1.9	1.8	1.7	1.6	0.7	1.0	0.4	0.7	0.3
106	SO_2NCO^+	8.7	8.5	7.0	7.2	4.2	4.1	4.4	3.8	2.0	3.4	1.4	1.5	0.6
141	$ClSO_2NCO^{\bullet+}$	2.0	2.1	2.0	1.9	1.5	1.4	1.3	1.2		0.7	0.0		

[a]Only fragments that contribute with more than 0.1% are included. [b]The relative intensities correspond to the sum of the abundances of the isotopologues of each fragment.

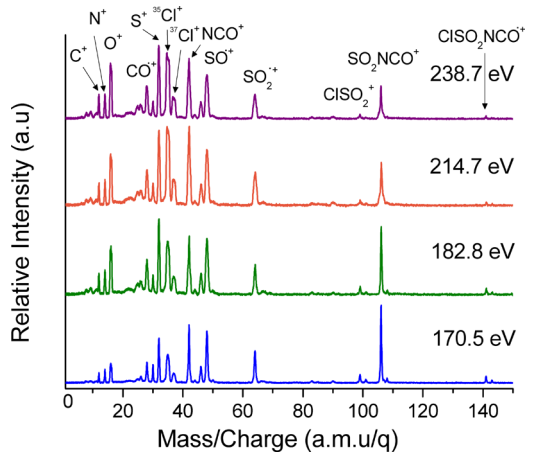

Figure 5. PEPICO spectra of $ClSO_2NCO$ taken in the S 2p, Cl 2p, and S 2s shallow-shell energy regions.

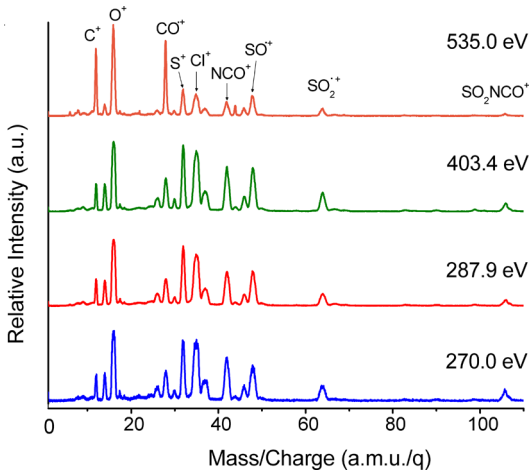

Figure 6. PEPICO spectra of $ClSO_2NCO$ taken in the C 1s, N 1s, and O 1s core-shell energy regions.

$S^{\bullet+}/NCO^+$ Coincidence. The most plausible mechanism for this coincidence, which reproduces the experimental slope of −1.5, is a SD-DCS initiated by the rupture of the Cl−S bond, as depicted in eq 7.

$$ClSO_2NCO^{2+} \rightarrow Cl^{\bullet} + SO_2NCO^{\bullet 2+}$$
$$SO_2NCO^{\bullet 2+} \rightarrow SO_2^{\bullet +} + \mathbf{NCO^+}$$
$$SO_2^{\bullet +} \rightarrow O + SO^{\bullet +}$$
$$SO^{\bullet +} \rightarrow O + \mathbf{S^{\bullet +}} \quad (7)$$

$S^{\bullet+}/Cl^+$ Coincidence. This coincidence, depicted in Figure 8 for the spectrum taken at 403.4 eV, is one of the most abundant islands in the whole energy range investigated. The approximately −2 experimental slope is well reproduced by a SD-DCS mechanism eq 8.

$$ClSO_2NCO^{2+} \rightarrow ClSO_2^{\bullet 2+} + NCO^{\bullet}$$
$$ClSO_2^{\bullet 2+} \rightarrow \mathbf{Cl^+} + SO_2^{\bullet +}$$
$$SO_2^{\bullet +} \rightarrow 2O + \mathbf{S^{\bullet +}} \quad (8)$$

$CO^{\bullet+}/Cl^+$ Coincidence. The experimental slope of −1.5 of this coincidence could only be explained through the mechanisms proposed in eq 9 ($\alpha_{theor} = -1.5$), which involve as a first step an atomic rearrangement to form the $ClNCO^{2+}$ species with the concomitant loss of SO_2.

DOI: 10.1021/acs.jpca.5b02396
J. Phys. Chem. A 2015, 119, 8021−8030

Table 3. Relative Intensity (%) of the Coincidence Island of the PEPIPICO Spectra of $ClSO_2NCO$ at Selected Photon Energies (eV)

	relative intensity (%)					
coincidence	182.8	214.7	238.7	270.0	403.4	535.4
$NCO^+/SO_2^{\bullet+}$	3.2	8.0	7.0	1.6	2.1	0.5
$NCO^+/SO^{\bullet+}$	8.8	9.7	10.9	3.7	4.2	1.4
$Cl^+/SO^{\bullet+}$	9.1	9.6	9.6	4.4	5.4	2.0
$S^{\bullet+}/NCO^+$	3.5	3.7	3.0	1.2	1.9	0.3
$S^{\bullet+}/Cl^+$	18.7	19.8	16.0	9.9	10.2	4.5
$CO^{\bullet+}/Cl^+$	4.4	4.6	3.5	3.5	4.8	1.3
$CO^{\bullet+}/S^{\bullet+}$	5.0	4.1	3.3	1.6	3.2	0.9
$O^{\bullet+}/SO^{\bullet+}$	3.4	2.6	1.5	1.0	2.6	0.6
$O^{\bullet+}/Cl^+$	12.8	11.6	14.3	24.6	23.9	13.7
$O^{\bullet+}/S^{\bullet+}$	17.7	15.1	21.3	34.0	21.1	18.8
$O^{\bullet+}/CO^{\bullet+}$	2.9	2.2	2.3	1.9	3.4	7.2
$C^{\bullet+}/Cl^+$	2.4	2.1	1.9	1.8	4.0	1.3
$C^{\bullet+}/S^{\bullet+}$	3.6	2.9	2.4	2.1	3.7	1.9
$C^{\bullet+}/O^{\bullet+}$	4.6	4.0	3.0	8.6	9.5	45.5

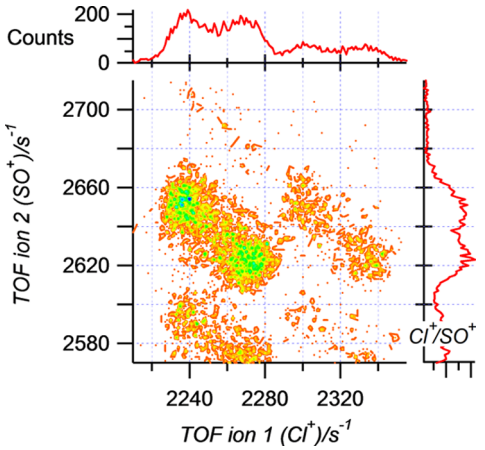

Figure 7. Contour map of the $Cl^+/SO^{\bullet+}$ coincidence island in the PEPIPICO spectrum of $ClSO_2NCO$ recorded at 403.4 eV.

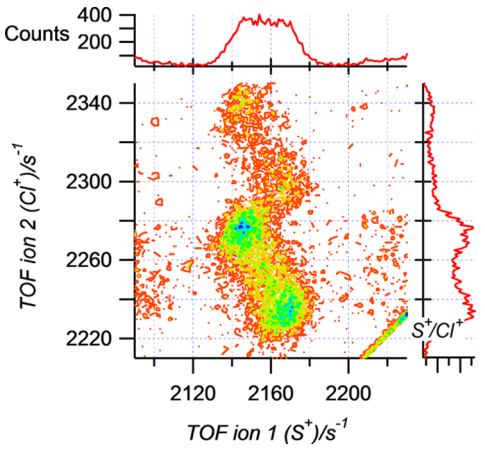

Figure 8. Contour map of the $S^{\bullet+}/Cl^+$ coincidence island in the PEPIPICO spectrum of $ClSO_2NCO$ recorded at 403.4 eV.

$$ClSO_2NCO^{2+} \rightarrow SO_2 + ClNCO^{2+}$$
$$ClNCO^{2+} \rightarrow \mathbf{Cl^+} + NCO^+$$
$$NCO^+ \rightarrow N^{\bullet} + \mathbf{CO^{\bullet+}} \quad (9)$$

The analogous coincidence, $CO^{\bullet+}/F^+$, was not observed for the FSO_2NCO molecule studied previously, indicating another difference between the behavior of the Cl− and F− derivatives.

$CO^{\bullet+}/S^{\bullet+}$ Coincidence. The value of the experimental slope of this island is −0.8. The only mechanism able to reproduce this value is a competitive secondary decay, CSD, schematized in eq 10, that predicts a theoretical slope of −0.79, in complete agreement with the experimental one.

$$ClSO_2NCO^{2+} \rightarrow ClSO_2^+ + NCO^+$$
$$NCO^+ \rightarrow N^{\bullet} + \mathbf{CO^{\bullet+}}$$
$$ClSO_2^+ \rightarrow Cl^{\bullet} + SO_2^{\bullet+}$$
$$SO_2^{\bullet+} \rightarrow 2O + \mathbf{S^{\bullet+}} \quad (10)$$

$O^{\bullet+}/SO^{\bullet+}$ Coincidence. In principle, the $O^{\bullet+}$ fragment of this coincidence can arise from either $-SO_2-$ or −NCO groups. However, the experimental slope ($\alpha_{exp} = -1$) of the $O^{\bullet+}/SO^{\bullet+}$ coincidence, presented in Figure 9 for the spectrum taken with

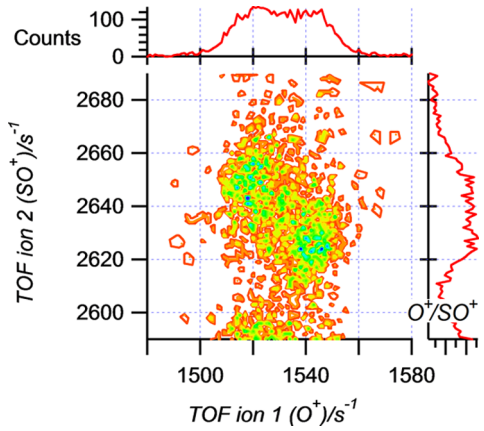

Figure 9. Contour map of the $O^{\bullet+}/SO^{\bullet+}$ coincidence island in the PEPIPICO spectrum of $ClSO_2NCO$ recorded at 403.4 eV.

403.4 eV, could only be reproduced by the four-body DCS mechanisms schematized by eq 11, revealing that the $O^{\bullet+}$ atomic fragment proceeds from the $-SO_2-$ group.

$$ClSO_2NCO^{2+} \rightarrow ClSO_2^{\bullet 2+} + NCO^{\bullet}$$
$$ClSO_2^{\bullet 2+} \rightarrow Cl^{\bullet} + SO_2^{2+}$$
$$SO_2^{2+} \rightarrow \mathbf{O^{\bullet+}} + \mathbf{SO^{\bullet+}} \quad (11)$$

$O^{\bullet+}/Cl^+$ Coincidence. The value of the experimental slope of approximately −1 for this coincidence island (see Figure 10) is well reproduced for at least two different mechanisms, a concerted fragmentation and a CSD channel, depicted in eq 12, that predict a theoretical slope of −0.93.

$$ClSO_2NCO^{2+} \rightarrow ClSO_2^+ + NCO^+$$
$$ClSO_2^+ \rightarrow \mathbf{Cl^+} + SO_2$$
$$NCO^+ \rightarrow \mathbf{O^{\bullet+}} + NC^{\bullet} \quad (12)$$

$O^{\bullet+}/S^{\bullet+}$ Coincidence. The island originated by the fragmentation of $ClSO_2NCO$ in $O^{\bullet+}$ and $S^{\bullet+}$ ions together with nondetected neutral fragments, depicted in Figure 11 for the spectrum recorded at 403.4 eV, presents an experimental slope close to −0.4. A SD-DCS mechanism described by eq 13, with a

DOI: 10.1021/acs.jpca.5b02396
J. Phys. Chem. A 2015, 119, 8021−8030

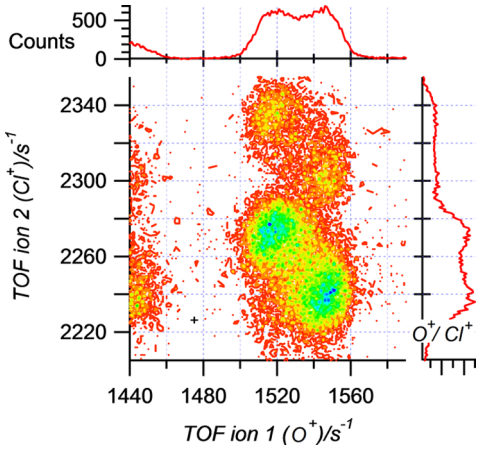

Figure 10. Contour map of the $O^{\bullet+}/Cl^{+}$ coincidence island in the PEPIPICO spectrum of $ClSO_2NCO$ recorded at 403.4 eV.

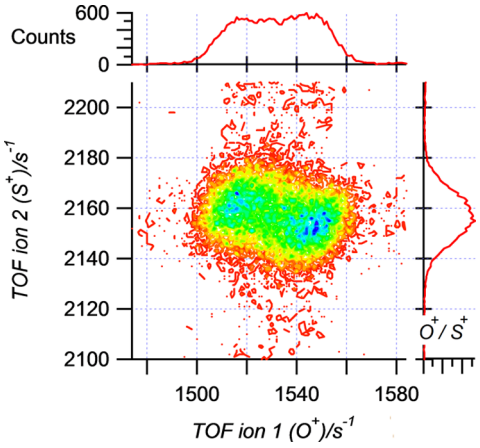

Figure 11. Contour map of the $O^{\bullet+}/S^{\bullet+}$ coincidence island in the PEPIPICO spectrum of $ClSO_2NCO$ recorded at 403.4 eV.

theoretical slope value of −0.39, is the one that better described the experimental findings.

$$ClSO_2NCO^{2+} \rightarrow ClSO_2{}^{\bullet 2+} + NCO^{\bullet}$$
$$ClSO_2{}^{\bullet 2+} \rightarrow \mathbf{O}^{\bullet+} + ClSO^{+}$$
$$ClSO^{+} \rightarrow O + Cl^{\bullet} + \mathbf{S}^{\bullet+} \quad (13)$$

$O^{\bullet+}/CO^{\bullet+}$ Coincidence. The experimental slope of about −0.7 of this island coincides very well with the $\alpha_{theo} = -0.67$ for the SD-DCS mechanism presented in eq 14. The same mechanism was proposed for this coincidence in the study of the fragmentation of FSO_2NCO in similar conditions, for which the experimental slope of also −0.7 was observed.[6]

$$ClSO_2NCO^{2+} \rightarrow ClSO^{\bullet} + ONCO^{\bullet 2+}$$
$$ONCO^{\bullet 2+} \rightarrow \mathbf{O}^{\bullet+} + NCO^{+}$$
$$NCO^{+} \rightarrow N^{\bullet} + \mathbf{CO}^{\bullet+} \quad (14)$$

$C^{\bullet+}/Cl^{+}$ Coincidence. The $\alpha_{exp} = -2.4$ for this island can only be explained through a SD-DCS mechanism involving a preliminary rearrangement channel, with $\alpha_{theo} = -2.3$, as schematized in eq 15.

$$ClSO_2NCO^{2+} \rightarrow ClCO^{\bullet 2+} + \text{neutral fragments}$$
$$ClCO^{\bullet 2+} \rightarrow \mathbf{Cl}^{+} + CO^{\bullet+}$$
$$CO^{\bullet+} \rightarrow \mathbf{C}^{\bullet+} + O \quad (15)$$

$C^{\bullet+}/S^{\bullet+}$ Coincidence. The experimental slope of about −1 of this island can be satisfactorily explained through the mechanism schematized in eq 16, for which $\alpha_{theo} = -1.1$ is predicted.

$$ClSO_2NCO^{2+} \rightarrow ClSO_2{}^{+} + NCO^{+}$$
$$ClSO_2{}^{+} \rightarrow \mathbf{S}^{\bullet+} + \text{neutral fragments}$$
$$NCO^{+} \rightarrow \mathbf{C}^{\bullet+} + \text{neutral fragments} \quad (16)$$

$C^{\bullet+}/O^{\bullet+}$ Coincidence. As well as observed in the study of FSO_2NCO, the $O^{\bullet+}$ fragment formed together with the $C^{\bullet+}$ ion arises from the −NCO group, as determined by the comparison of the approximately −2.2 value of the island's experimental slope with the $\alpha_{theo} = -2.2$ for the SD-DCS mechanisms depicted in eq 17.

$$ClSO_2NCO^{2+} \rightarrow ClSO_2{}^{\bullet} + NCO^{\bullet 2+}$$
$$NCO^{\bullet 2+} \rightarrow \mathbf{O}^{\bullet+} + NC^{+}$$
$$NC^{+} \rightarrow N^{\bullet} + \mathbf{C}^{\bullet+} \quad (17)$$

CONCLUSION

The main fragmentation mechanism of $ClSO_2NCO$ excited with photons in the valence energy region, between 12 and 21 eV, occurs through the rupture of the Cl−S single bond, forming the SO_2NCO^{+} fragment. This mechanism contrasts with the one observed for the related FSO_2NCO, in which the rupture of the S−N bond originates the $FSO_2{}^{+}$ fragment.[6] As explained before, this difference may be attributed to the different outermost electronic properties of these species, represented by the character of the HOMOs of both molecules, as determined by photoelectron spectroscopy and theoretical calculations.

After electronic decay of the core or shallow excited or ionized $ClSO_2NCO$, the molecule fragments following several different unimolecular mechanisms, detected as coincidence islands in the bidimensional PEPIPICO spectra. Three of the mechanisms initiate with the rupture of the Cl−S bond, giving in all the cases neutral chlorine radical and the $SO_2NCO^{\bullet 2+}$ fragment. Subsequent fragmentation of this species originates the $NCO^{+}/SO_2{}^{\bullet+}$, $NCO^{+}/SO^{\bullet+}$, and $S^{\bullet+}/NCO^{+}$ coincidences. The second group of mechanisms involves the S−N bond breaking as the first step. In this case the double charge can remain in only one of the fragments, or distributed on each of them. If the double charge remains on $ClSO_2{}^{2+}$, the subsequent evolution of this intermediate originates the $Cl^{+}/SO^{\bullet+}$, $Cl^{+}/S^{\bullet+}$, $O^{\bullet+}/SO^{\bullet+}$, and $O^{\bullet+}/S^{\bullet+}$ coincidences. If the charge distributes on each fragment after the S−N bond rupture, giving $ClSO_2{}^{+}$ and NCO^{+}, the $CO^{\bullet+}/S^{\bullet+}$, $O^{\bullet+}/Cl^{+}$, and $C^{\bullet+}/S^{\bullet+}$ pairs are detected in coincidence. In only one case the double charge remains in the NCO^{2+} fragment, which follows fragmentation ended in the $C^{\bullet+}/O^{\bullet+}$ coincidence. A third type of coincidence island can only be explained with an initial atomic rearrangement. $ClNCO^{2+}$ was proposed as the intermediate of the $CO^{\bullet+}/Cl^{+}$ pair, while $ONCO^{2+}$ and $ClCO^{2+}$ were proposed as precursors of the $O^{\bullet+}/CO^{\bullet+}$ and $C^{\bullet+}/Cl^{+}$ pairs, respectively. It is interesting to remark that the photolysis of chlorosulfonyl isocyanate excited with light between 12 and 550 eV is a source of chlorine radicals, through a

DOI: 10.1021/acs.jpca.5b02396
J. Phys. Chem. A 2015, 119, 8021−8030

number of different mechanisms for each region (see, for instance, eqs 1 to 5, 7, 10, 11, and 13).

AUTHOR INFORMATION

Corresponding Author

*E-mail: romano@quimica.unlp.edu.ar.

Notes

The authors declare no competing financial interest.

ACKNOWLEDGMENTS

This work has been largely supported by the Brazilian Synchrotron Light Source (LNLS), under proposals TGM-12776 and SGM-11670. The authors wish to thank Arnaldo Naves de Brito and his research group for fruitful discussions and generous collaboration during their several stays in Campinas and the TGM and SGM beamline staffs for their assistance throughout the experiments. They also are indebted to the Agencia Nacional de Promoción Científica y Tecnológica (ANPCyT), Consejo Nacional de Investigaciones Científicas y Técnicas (CONICET), and the Facultad de Ciencias Exactas, Universidad Nacional de La Plata, for financial support.

REFERENCES

(1) Bava, Y. B.; Berrueta Martínez, Y.; Moreno Betancourt, A.; Erben, M. F.; Cavasso Filho, R. L.; Della Védova, C. O.; Romano, R. M. Ionic Fragmentation Mechanisms of 2,2,2-Trifluoroethanol Following Excitation with Synchrotron Radiation. *ChemPhysChem* **2015**, *16*, 322−330.

(2) Romano, R. M.; Della Védova, C. O.; Beckers, H.; Willner, H. Photochemistry of $SO_2/Cl_2/O_2$ Gas Mixtures: Synthesis of the New Peroxide $ClSO_2OOSO_2Cl$. *Inorg. Chem.* **2009**, *48*, 1906−1910.

(3) Romano, R. M.; Della Védova, C. O.; Downs, A. J.; Greene, T. M. Matrix Photochemistry of *syn*-(Chlorocarbonyl)sulfenyl Bromide, *syn*-ClC(O)SBr: Precursor to the Novel Species *anti*-ClC(O)SBr, *syn*-BrC(O)SCl, and BrSCl. *J. Am. Chem. Soc.* **2001**, *123*, 5794−5801.

(4) Gómez Castaño, J. A.; Romano, R. M.; Beckers, H.; Willner, H.; Della Védova, C. O. Formation of the Matrix Isolated Difluoromethylselanes XCF_2SeH, with X = H, Cl, Through Photolysis of Selenoacetic *Se*-acids, $XCF_2C(O)SeH$. *Eur. J. Inorg. Chem.* **2013**, *2013*, 4585−4594.

(5) Robles, N. L.; Flores Antognini, A.; Romano, R. M. Formation of XNCO Species (X = F, Cl) Through Matrix-Isolation Photochemistry of XSO_2NCO Molecules. *J. Photochem. Photobiol., A* **2011**, *223*, 194−201.

(6) Moreno Betancourt, A.; Flores Antognini, A.; Erben, M. F.; Cavasso Filho, R. L.; Tong, S.; Ge, M.; Della Védova, C. O.; Romano, R. M. Electronic Properties of Fluorosulfonyl Isocyanate, FSO_2NCO: A Photoelectron Spectroscopy and Synchrotron Photoionization Study. *J. Phys. Chem. A* **2013**, *117*, 9179−9188.

(7) Dhar, D. N.; Dhar, P. *The Chemistry of Chlorosulfonyl Isocyanate*; World Scientific Publishing Co. Pte. Ltd.: United Kingdom, 2002.

(8) Álvarez, R. M. S.; Cutin, E. H.; Della Védova, C. O. Conformational and Bond Properties of Chlorosulfonyl Isocyanate, $ClSO_2NCO$. *Spectrochim. Acta, Part A* **1995**, *51A*, 555−561.

(9) Durig, J. R.; Zhou, L.; Gounev, T. K.; Guirgis, G. A. Vibrational Spectra, Conformational Stability and Ab Initio Calculations of Chlorosulfonyl Isocyanate. *Spectrochim. Acta, Part A* **1997**, *53*, 1581−1593.

(10) Brunvoll, J.; Hargittai, I.; Seip, R. Electron-Diffraction Investigation of the Molecular Structure of Sulphonyl Chloride Isocyanate. *J. Chem. Soc., Dalton Trans.* **1978**, *7*, 299−302.

(11) Fengyi, L.; Xiaoqing, Z.; Weigang, W.; Lingpeng, M.; Shijun, Z.; Maofa, G.; Dianxun, W. Photoelectron Spectra and Electronic Structures of Some Chlorosulfonyl Pseudohalides. *Spectrochim. Acta, Part A* **2006**, *63*, 111−116.

(12) Lira, A. C.; Rodrigues, A. R. D.; Rosa, A.; Gonçalves da Silva, C. E. T.; Pardine, C.; Scorzato, C.; Wisnivesky, D.; Rafael, F.; Franco, G. S.; Tosin, G.; et al. *First Year Operation of the Brazilian Sinchrotron Light Source*; European Particle Accelerator Conference, 1998, Stockholm.

(13) Fonseca, P. de T.; Pacheco, J. G.; d'A Samogin, E.; de Castro, A. R. B. Vacuum Ultraviolet Beam Lines at Laboratório Nacional de Luz Síncrotron, the Brazilian Synchrotron Source. *Rev. Sci. Instrum.* **1992**, *63*, 1256−1259.

(14) Burmeister, F.; Coutinho, L. H.; Marinho, R. R. T.; Homem, M. G. P.; de Morais, M. A. A.; Mocellin, A.; Björneholm, O.; Sorensen, S. L.; Fonseca, P. T.; Lindgren, A.; et al. Description and Performance of an Electron-Ion Coincidence TOF Spectrometer Used at the Brazilian Synchrotron Facility LNLS. *J. Electron Spectrosc. Relat. Phenom.* **2010**, *180*, 6−13.

(15) Cavasso Filho, R. L.; Homem, M. G. P.; Landers, R.; Naves de Brito, A. Advances on the Brazilian Toroidal Grating Monochromator (TGM) Beamline. *J. Electron Spectrosc. Relat. Phenom.* **2005**, *144−147*, 1125−1127.

(16) Cavasso Filho, R. L.; Lago, A. F.; Homem, M. G. P.; Pilling, S.; Naves de Brito, A. Delivering High-Purity Vacuum Ultraviolet Photons at the Brazilian Toroidal Grating Monochromator (TGM) Beamline. *J. Electron Spectrosc. Relat. Phenom.* **2007**, *156−158*, 168−171.

(17) Cavasso Filho, R. L.; Homen, M. G. P.; Fonseca, P. T.; Naves de Brito, A. A Synchrotron Beamline for Delivering High Purity Vacuum Ultraviolet Photons. *Rev. Sci. Instrum.* **2007**, *78*, 115104.

(18) Kivimaki, A.; Alvarez Ruiz, J.; Erman, P.; Hatherly, P.; Melero García, E.; Rachlew, E.; Rius i Riu, J.; Stankiewicz, M. An Energy Resolved Electron−Ion Coincidence Study Near the S 2p Thresholds of the SF_6 Molecule. *J. Phys. B: At., Mol. Opt. Phys.* **2003**, *36*, 781−791.

(19) Frasinski, L. J.; Stankiewicz, M.; Randall, K. J.; Hatherly, P. A.; Codling, K. Dissociative Photoionisation of Molecules Probed by Triple Coincidence; Double Time-of-Flight Techniques. *J. Phys. B: At. Mol. Phys.* **1986**, *19*, L819−L824.

(20) Eland, J. H. D.; Wort, F. S.; Royds, R. N. A Photoelectron-Ion-Ion Triple Coincidence Technique for the Study of Double Photoionization and its Consequences. *J. Electron Spectrosc. Relat. Phenom.* **1986**, *41*, 297−309.

(21) Naves de Brito, A.; Feifel, R.; Mocellin, A.; Machado, A. B.; Sundin, S.; Hjelte, I.; Sorensen, S. L.; Björneholm, O. Femtosecond Dissociation Dynamics of Core Excited Molecular Water. *Chem. Phys. Lett.* **1999**, *309*, 377−385.

(22) Frisch, M. J.; Trucks, G. W.; Schlegel, H. B.; Scuseria, G. E.; Robb, M. A.; Cheeseman, J. R.; Montgomery, J. A., Jr.; Vreven, T.; Kudin, K. N.; Burant; et al. *Gaussian 03, Revision B.04*; Gaussian, Inc.: Pittsburgh, PA, 2003.

(23) Cooper, G.; Zarate, E. B.; Jones, R. K.; Brion, C. E. Absolute Oscillator Strengths for Photoabsorption, Photoionization and Ionic Photofragmentation of Sulphur Dioxide. II. The S 2p and 2s Inner Shells. *Chem. Phys.* **1991**, *150*, 251−261.

(24) Sze, K. H.; Brion, C. E.; Tronc, M.; Bodeur, S.; Hitchcock, A. P. Inner and Valence Shell Electronic Excitation of Dimethyl Sulfoxide by Electron Energy Loss and Photoabsorption Spectroscopies. *Chem. Phys.* **1988**, *121*, 279−297.

(25) Eland, J. H. D. The Dynamics of Three-Body Dissociations of Dications Studied by the Triple Coincidence Technique PEPIPICO. *Mol. Phys.* **1987**, *61*, 725−745.

DOI: 10.1021/acs.jpca.5b02396
J. Phys. Chem. A 2015, 119, 8021−8030